

Bi(111) Thin Film with Insulating Interior but Metallic Surfaces

Shunhao Xiao, Dahai Wei, and Xiaofeng Jin*

State Key Laboratory of Surface Physics and Department of Physics, Fudan University, Shanghai 200433, China

(Received 5 June 2012; published 17 October 2012)

The electrical conductance of epitaxial Bi thin films grown on BaF₂(111) by molecular beam epitaxy has been systematically investigated as a function of both film thickness (4–540 nm) and temperature (5–300 K). Unlike bulk Bi as a prototypical semimetal, the Bi thin films up to 90 nm are found to be insulating in the interior but metallic on the surface. This finding not only has unambiguously resolved the long-standing controversy about the existence of the semimetal-semiconductor transition in Bi thin films but also provided a straightforward interpretation for the perplexing temperature dependence of the resistivity of Bi thin films, which in turn might have some potential applications in spintronics.

DOI: [10.1103/PhysRevLett.109.166805](https://doi.org/10.1103/PhysRevLett.109.166805)

PACS numbers: 73.25.+i, 71.30.+h, 73.50.–h

Bi is a pentavalent element in the periodic table with the atomic structure of [Xe]4f¹⁴5d¹⁰6s²6p³. It crystallizes in a rhombohedral (A15) structure with two ions and ten valence electrons per primitive cell. The even number of valence electrons makes it very close to being an insulator, but the very slight overlap between the conduction and valence bands eventually drives it to a prototype semimetal with a very small number of carriers ($3 \times 10^{17} \text{ cm}^{-3}$), therefore leading to an unusually long Fermi wavelength (30 nm) [1,2]. Along with small effective carrier masses and an unconventionally long carrier mean free path, Bi as a bulk material has distinguished itself from the rest of elements in the periodic table [3].

With the given special properties of bulk Bi, it is even more interesting and appealing to manipulate its electronic structure in thin films to switch Bi from a semimetal to an insulator or semiconductor. To achieve this goal, it has been proposed theoretically that the quantum size effect could indeed drive a semimetal to semiconductor transition in thin films when the thicknesses are comparable to the Fermi wavelength [4,5]. Despite considerable experimental effort in the last five decades, however, such a transition has not been clearly established [2,6–9]. Especially, the experimentally observed nonmonotonic temperature dependence of the electrical resistivity does not fit at all the physical picture anticipated by the existence of a semiconductor phase [10–13]. It was argued recently by Hirahara *et al.*, by means of angle resolved photoemission spectroscopy, that Bi(111) films should always be metallic because of the persistence of thickness-independent metallic surface states, in direct contrast to the semimetal-semiconductor transition; meanwhile the room temperature electrical transport was also conducted to confirm the existence of the metallic surface states but failed to realize the semiconducting nature of the Bi thin films [14,15]. Therefore, the existence of a semimetal-semiconductor transition in Bi films remains elusive.

In this Letter, we demonstrate unambiguously the coexistence of the semiconducting and metallic phases in MBE

grown thin films (< 90 nm) and further confirm that the former arises from the quantum confinement of the interior and the latter from the surface states. Our results shed light on the long-standing issue of the semimetal-semiconductor transition in Bi films, which also opens up a possibility to explore the topological properties of Bi [16–18] and Bi-based topological insulators [19–21].

Single crystalline Bi(111) films ranging from 4 to 540 nm thick were epitaxially grown on BaF₂(111) by molecular-beam epitaxy in an ultrahigh vacuum system equipped with reflection high energy electron diffraction (RHEED) and Auger electron spectroscopy (AES) [22]. Clean and ordered BaF₂(111) substrates were first prepared by annealing at 700 °C for 10 minutes then cooled down and kept at 70 °C, on which the epitaxial growth of Bi was followed while the evaporation rate was monitored by a quartz microbalance. To prevent oxidation in ambient air during the transport measurement, a 6 nm MgO capping layer was deposited on each sample before taken out from the UHV chamber. The grazing angle x-ray diffraction (XRD) experiment was performed at the Beijing Synchrotron Radiation Facility [23]. The transport measurements were carried out on the samples patterned into standard Hall bars along the [11 $\bar{2}$] direction, using the Quantum Design physical property measurement system (PPMS-9T) [24].

Figure 1 shows a set of representative RHEED and grazing angle XRD results for Bi/BaF₂(111) of different film thicknesses, which clearly indicates that the epitaxial growth of Bi on BaF₂(111) involves two stages. In the early stage below about 15 nm, the RHEED patterns (as for 6 nm thick film) are complicated, implying that the Bi films grow in a polycrystal. This is confirmed by the XRD result which shows the coexistence of the Bi pseudocubic phase [(100) peak at 27.1 degree] and Bi hexagonal phase [(1100) peak at 39.7 degree] in Figs. 1(b) and 1(c), respectively. In the later stage of film growth beyond 15 nm, the RHEED patterns (as for 25 nm thick film) become very simple, implying that the Bi films grow in a single crystal. This

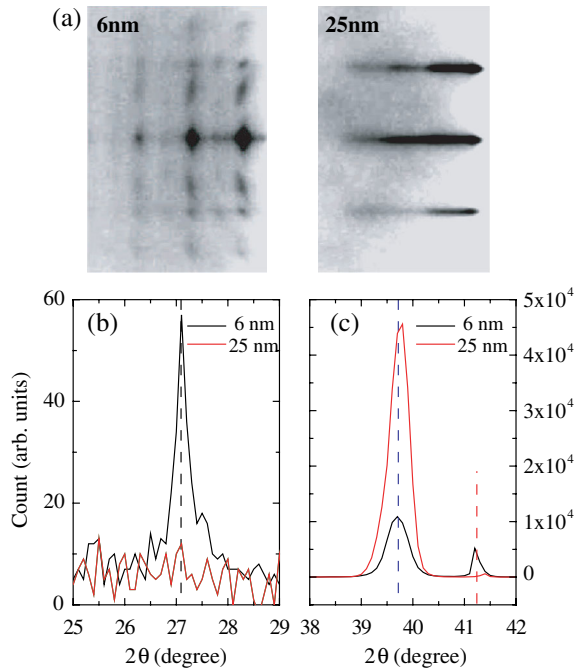


FIG. 1 (color online). (a) RHEED patterns of 6 and 25 nm of Bi on BaF_2 ; the incident electron beam is along the $[11\bar{2}]$ direction of BaF_2 . (b),(c) The grazing angle XRD spectra of the same samples; the small peak around 41° comes from the $(0\bar{2}2)$ diffraction of the BaF_2 substrate.

is again revealed by XRD that the pseudocubic phase has disappeared and transformed completely to the hexagonal phase of Bi(111) as seen in Figs. 1(b) and 1(c). In fact, the overall growth behavior observed here is a quite generic feature specific for the epitaxial growth of Bi on various substrates (Si, HOPG, and others) [25,26], although the transformation from the polycrystalline pseudocubic to single crystalline hexagonal phase happens at different film thicknesses for different substrates. In the case of Bi/Si(111) – (7×7) , a textured pseudocubic Bi phase was realized at the initial stage of growth, followed by a mixture with a hexagonal Bi phase, and finally the entire film transformed into a pure hexagonal epitaxial Bi phase [25]. It was further proposed that after the early coalescence of pseudocubic Bi islands, a small number of lattice-matched hexagonal nuclei trigger and thrust the transformation both in the structure (pseudocubic to hexagonal) and in crystallinity (textured to single crystalline) [26]. We therefore conclude that we can obtain experimentally pure Bi(111) single crystal films thicker than 15 nm on $\text{BaF}_2(111)$.

Figure 2(a) shows the electrical conductance of Bi as a function of film thickness measured at different temperatures, where three distinct regimes, as marked, can be realized. In regime (I) the conductance is extremely small reflecting the well-known insulating nature of the pseudocubic phase of Bi [15]. Regime (II) corresponds to the mixture of both pseudocubic and hexagonal phases of Bi,

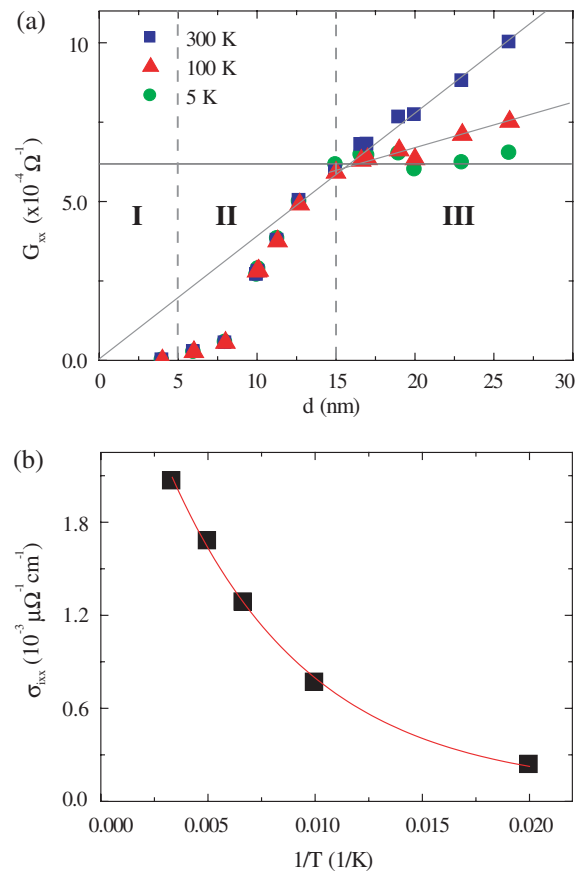


FIG. 2 (color online). (a) Conductance as a function of the sample thickness at 300, 100, and 5 K. (b) Conductivity of the film interior derived from the slopes of the conductance-thickness lines in region (III) of (a) as a function of temperature. The curve is an exponential fitting.

and the transformation from the former to the latter. The most interesting and surprising result lies in regime (III), where the conductance exhibits strong temperature dependence. It is noted that at 5 K the conductance remains almost unchanged with increasing Bi film thickness from 15 to 25 nm; i.e., the additional 10 nm Bi does not contribute at all to the electrical conductance; this in turn strongly implies that the low temperature electrical transport in Bi films should be dominated by the metallic surface states while the corresponding film interiors are insulating. In contrast to the 5 K case the conductance at 300 K increases linearly as a function of film thickness, which suggests that besides the surface channel the electron transport in the film interior has also contributed to the conductance. However, this is possible only when the film interior is an insulator or a semiconductor with a very small energy gap of about 20 meV. Then it would behave like an insulator at low temperature (e.g., 5 K) because of the energy gap, but would become conducting at higher temperatures (e.g., 300 K) when the thermal excitation from the valence band to conduction band is no longer

negligible. Therefore, this is the first direct experimental evidence for the existence of the long debated insulating or semiconducting phase in Bi films, yet the physical picture turns out to be more complicated than what was originally proposed. It is clear now that Bi(111) thin films with thicknesses comparable with the Fermi wavelength are indeed insulating or semiconducting but only in the film interiors, yet their surfaces are always metallic.

Now we turn to estimate quantitatively the energy band gap of the Bi(111) film interior. Because of the two channels for the total conductance—the surface and interior contributions—we have:

$$G_{xx} = G_s + \sigma_{ixx} \frac{w}{l} d. \quad (1)$$

G_{xx} and G_s are the total and surface conductances, respectively, and σ_{ixx} is the conductivity of the film interior; d , l , w are the thickness, length, and width of the Bi(111) Hall bar, respectively. In Eq. (1) G_{xx} is proportional to d at any given temperature where σ_{ixx} is just a temperature-dependent constant. This equation describes the linear dependence of the conductivity in the thickness range of 15–25 nm in Fig. 2(a). The slopes of the straight lines are the conductivity of the films and it is plotted in Fig. 2(b). With the slopes at different temperatures, we further establish a relation between σ_{ixx} and temperature, as shown in Fig. 2(b) as σ_{ixx} vs $1/T$. The set of data can be well fitted by an exponential function $\alpha e^{-(\Delta E/2kT)}$, here α being a constant and ΔE an energy gap, while k and T are the Boltzmann constant and temperature, respectively. The fitting to the activated conductivity gives an energy gap of $\Delta E = 24$ meV. Clearly when $kT \ll \Delta E$, e.g., at 5 K, the interior of the film is insulating, but when $kT \sim \Delta E$, the film turns to be conducting.

After identifying the semiconductor phase in single crystalline Bi films, we now try to find out how thin a Bi(111) film would undergo the semimetal-semiconductor transition. In Fig. 3(a), we show the conductivity vs temperature curves for different film thicknesses, which have been normalized with the value at 300 K. The inset clearly shows that the slope of the curves does change sign from negative to positive as the thickness is decreased—direct and strong evidence for the semimetal to semiconductor transition in Bi thin films. By plotting the temperature coefficient of conductivity around 300 K ($\frac{\sigma_{300\text{K}} - \sigma_{270\text{K}}}{\sigma_{300\text{K}} \times 30\text{K}}$) as a function of film thickness in Fig. 3(b), we find that the temperature coefficient crosses over zero at about 90 nm, an indication of the semimetal to semiconductor transition in Bi(111) films. Presumably due to the poor sample quality, especially the surface quality, what was missed in Ref. [6] is the well-defined bump appearing at thinner Bi film thicknesses as clearly seen in Fig. 3(b) in our MBE grown single crystalline films. The appearance of the bump is in fact a result of the competition between the metallic surface and the semiconductor interior of the Bi(111) thin film according to Eq. (1), as the relative weight of the former gradually

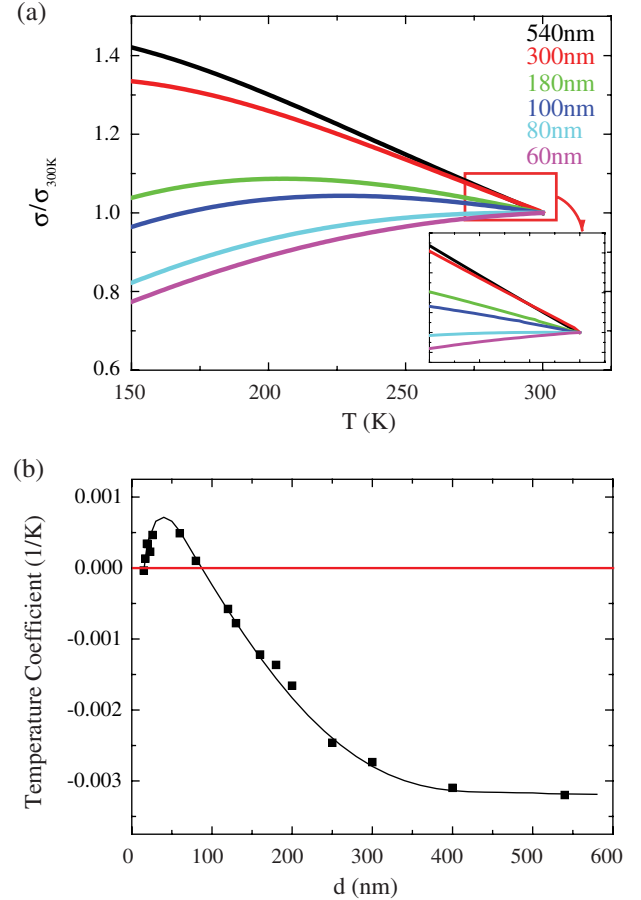


FIG. 3 (color online). (a) Conductivity-temperature curves (540–60 nm from top to bottom) normalized with the value at 300 K. The inset is a zoom-in from 270 to 300 K. (b) The temperature coefficients of conductivity between 270 and 300 K as a function of sample thicknesses. The black curve is a guide to the eye.

increases and eventually dominates as the film thickness decreases.

With this new model, we try to further analyze the effect of the thickness on the overall temperature dependence of the conductivity, and clarify the long-standing puzzle about the nonmonotonic behavior of the conductivity vs temperature curve in Bi films. Similar to Eq. (1), the total conductivity σ_{xx} from the two (surface and film interior) channels can be expressed as

$$\sigma_{xx} = \frac{\sigma_s}{d} + \alpha e^{-(\Delta E/2kT)}. \quad (2)$$

Here σ_s is the surface conductivity. According to the Matthiessen's rule, it can be further expressed in resistivity as $\sigma_s = \frac{1}{(\rho_0 + \rho_T)}$, where ρ_0 and ρ_T are the surface residual and electron-phonon induced resistivity. By adopting the results in the literature for the surface electron-phonon induced resistivity $\rho_T = sT$ [27], and the quantum size effect induced energy gap $\Delta E = \frac{2b}{d^2}$ (b is a constant) [4,5], Eq. (2) turns into

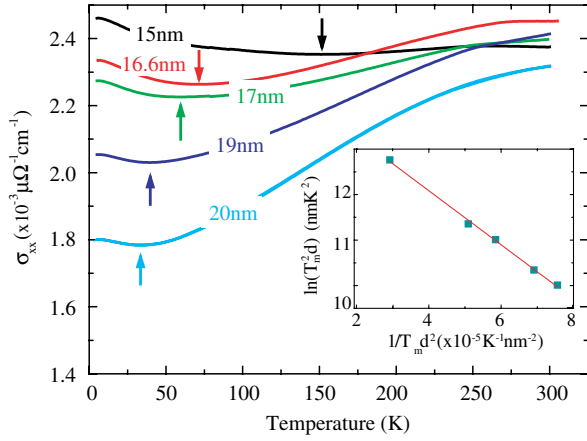


FIG. 4 (color online). Temperature dependent conductivities of samples with different thickness. The inset shows $\ln(T_m^2 d)$ as a function of $1/T_m d^2$.

$$\sigma_{xx} = \frac{1}{d(\rho_0 + sT)} + \alpha e^{-b/(kTd^2)}. \quad (3)$$

For a given sample with fixed film thickness, it is obvious that the first term from the metallic surface would decrease as the sample temperature increases, but in contrast the second term from the semiconductor interior would increase. It is exactly this competition that caused the nonmonotonic behavior of the temperature dependent conductivity or resistivity. Depending on the Bi film thickness, when the two terms are comparable in magnitude, a valley in conductivity should be expected in principle, which would qualitatively explain the experimentally observed phenomena in Fig. 4. The appearance of the film thickness and temperature in both the denominator of the first term and exponent of the second results in a very complex behavior in the conductivity. Quantitatively, for each fixed film thickness the minimal point of the valley T_m can be determined by minimizing Eq. (3) while noticing the experimental fact that ρ_T is smaller than ρ_0 ; therefore, we reach the following equation:

$$\ln(T_m^2 d) = -\frac{b}{kT_m d^2} + \ln\left(\frac{\alpha b \rho_0^2}{sk}\right). \quad (4)$$

Clearly, as seen in the inset of Fig. 4, the experimental data of $\ln(T_m^2 d)$ vs $\frac{1}{T_m d^2}$ can be well fitted by a straight line with a slope of $-b/k \approx -6 \times 10^4 \text{ K} \cdot \text{nm}^2$, from which we get the film thickness dependent energy gaps of the semiconducting interiors: 46 meV for 15 nm and 26 meV for 20 nm Bi films, respectively. These not only agree very well with the foregoing obtained result deduced from Fig. 2(b) but also provide the trend of the thickness dependent energy gap of the film interiors in Bi.

In summary, we have demonstrated in this work that the long debated semimetal to semiconductor transition does happen in Bi(111) thin film when the film thickness is comparable to the Fermi wavelength of Bi; the problem

had been controversial because of the subtle fact that the film interior is semiconducting while the surface is always metallic.

This work was supported by MSTC (Grant No. 2009CB929203 and No. 2011CB921802), NSFC (Grant No. 10834001), MOE, and SCST. The technical support from Beijing Synchrotron Radiation Facility (BSRF) for XRD measurements is also acknowledged.

*Corresponding author: xfjin@fudan.edu.cn

- [1] N. W. Ashcroft and D. N. Mermin, *Solid State Physics* (Thomson Learning, Toronto, 1976), 1st ed.
- [2] P. Hofmann, *Prog. Surf. Sci.* **81**, 191 (2006).
- [3] L. A. Falkovski, *Sov. Phys. Usp.* **11**, 1 (1968).
- [4] V. N. Lutsii, *JETP Lett.* **2**, 245 (1965).
- [5] V. B. Sandomirskii, *Sov. Phys. JETP* **25**, 101 (1967).
- [6] V. P. Duggal, R. Rup, and P. Tripathi, *Appl. Phys. Lett.* **9**, 293 (1966).
- [7] C. A. Hoffman, J. R. Meyer, F. J. Bartoli, A. Di Venere, X. J. Yi, C. L. Hou, H. C. Wang, J. B. Ketterson, and G. K. Wong, *Phys. Rev. B* **48**, 11431 (1993).
- [8] H. T. Chu, *Phys. Rev. B* **51**, 5532 (1995).
- [9] C. A. Hoffman, J. R. Meyer, F. J. Bartoli, A. Di Venere, X. J. Yi, C. L. Hou, H. C. Wang, J. B. Ketterson, and G. K. Wong, *Phys. Rev. B* **51**, 5535 (1995).
- [10] R. A. Hoffman and D. R. Frankl, *Phys. Rev. B* **3**, 1825 (1971).
- [11] N. Garcia, Y. H. Kao, and M. Strongin, *Phys. Rev. B* **5**, 2029 (1972).
- [12] F. Y. Yang, K. Liu, K. Hong, D. H. Reich, P. C. Searson, and C. L. Chien, *Science* **284**, 1335 (1999).
- [13] M. Lu, R. J. Zieve, J. A. van Hulst, H. M. Jaeger, T. F. Rosenbaum, and S. Radelaar, *Phys. Rev. B* **53**, 1609 (1996).
- [14] T. Hirahara, T. Nagao, I. Matsuda, G. Bihlmayer, E. V. Chulkov, Y. M. Koroteev, P. M. Echenique, M. Saito, and S. Hasegawa, *Phys. Rev. Lett.* **97**, 146803 (2006).
- [15] T. Hirahara, I. Matsuda, S. Yamazaki, N. Miyata, S. Hasegawa, and T. Nagao, *Appl. Phys. Lett.* **91**, 202106 (2007).
- [16] S. Murakami, *Phys. Rev. Lett.* **97**, 236805 (2006).
- [17] J. W. Wells, F. M. J. H. Dil, J. Lobo-Checa, V. N. Petrov, J. Osterwalder, M. M. Ugeda, I. Fernandez-Torrente, J. I. Pascual, E. D. L. Rienks, M. F. Jensen *et al.*, *Phys. Rev. Lett.* **102**, 096802 (2009).
- [18] Z. Liu, C.-X. Liu, Y.-S. Wu, W.-H. Duan, F. Liu, and J. Wu, *Phys. Rev. Lett.* **107**, 136805 (2011).
- [19] L. Fu and C. L. Kane, *Phys. Rev. B* **76**, 045302 (2007).
- [20] D. Hsieh, D. Qian, L. Wray, Y. Xia, Y. S. Hor, R. J. Cava, and M. Z. Hasan, *Nature (London)* **452**, 970 (2008).
- [21] H. Zhang, C.-X. Liu, X.-L. Qi, X. Dai, Z. Fang, and S.-C. Zhang, *Nature Phys.* **5**, 438 (2009).
- [22] C. S. Tian *et al.*, *Phys. Rev. Lett.* **94**, 137210 (2005).
- [23] L. F. Yin, D. H. Wei, N. Lei, L. H. Zhou, C. S. Tian, G. S. Dong, X. F. Jin, L. P. Guo, Q. J. Jia, and R. Q. Wu, *Phys. Rev. Lett.* **97**, 067203 (2006).

- [24] Y. Tian, L. Ye, and X. Jin, *Phys. Rev. Lett.* **103**, 087206 (2009).
- [25] T. Nagao, J.T. Sadowski, M. Saito, S. Yaginuma, Y. Fujikawa, T. Kogure, T. Ohno, Y. Hasegawa, S. Hasegawa, and T. Sakurai, *Phys. Rev. Lett.* **93**, 105501 (2004).
- [26] S. Yaginuma, T. Nagao, J.T. Sadowski, M. Saito, K. Nagaoka, Y. Fujikawa, T. Sakurai, and T. Nakayama, *Surf. Sci.* **601**, 3593 (2007).
- [27] I. Matsuda, C. Liu, T. Hirahara, M. Ueno, T. Tanikawa, T. Kanagawa, R. Hobara, S. Yamazaki, S. Hasegawa, and K. Kobayashi, *Phys. Rev. Lett.* **99**, 146805 (2007).